



Solid-state structural elucidation and electrochemical analysis of uranyl naphthylsalophen

Journal:	<i>ChemComm</i>
Manuscript ID	CC-COM-06-2018-005242.R1
Article Type:	Communication

SCHOLARONE™
Manuscripts

Solid-state structural elucidation and electrochemical analysis of uranyl naphthylsalophen

Received 00th January 20xx,
Accepted 00th January 20xx

Julie E. Niklas,^a Emily E. Hardy,^a and Anne E. V. Gorden*^a

DOI: 10.1039/x0xx00000x

www.rsc.org/

A salophen ligand derivative incorporating naphthalene (naphthylsalophen = [H₂L]) and the corresponding uranyl (UO₂²⁺) complex have been synthesized and characterized both in solution and the solid-state. A hydrogen bonding uranyl tetramer and the electrochemical analysis of [H₂L] and UO₂[L] are described.

The coordination chemistry of uranium is dominated by uranyl U(VI) complexes as a result of the stability of the linear [O=U=O]²⁺ moiety; however, the study of lower-valent uranium complexes and multielectron processes has become of wide interest for applications in catalysis and nuclear waste remediation.¹ For example, the bio-immobilization of the highly water soluble U(VI) by reduction to the insoluble U(IV) is known to proceed through a key pentavalent intermediate, but this process is poorly understood.² U(V) species are generally unstable due to disproportionation, which complicates their isolation and characterization. Systems in which the U(VI)/U(V) redox couple can be studied are therefore, very useful in the development of an improved understanding of the reduction of uranyl and the impacts equatorial ligands have on the stabilization of U(V) (UO₂⁺) species. Efforts to more thoroughly describe the unique bonding and electronic properties of uranium have increased of late, with significant focus on oxo-functionalization of uranyl complexes, as this both displays the reactivity of the terminal oxo moieties, which were long considered to be inert, and allows for more facile reduction of the metal centre.³ Recently, pairing strongly donating equatorial ligands with Lewis acid acceptors has proven a useful route to oxo-functionalization and consequent reduction to UO₂⁺.^{3a, 4} Using a dipyrin derivative, the Arnold group demonstrated tunability of the nonaqueous U(VI)/U(V) and U(V)/U(IV) redox couples to ranges that are accessible to mild reducing agents.⁵

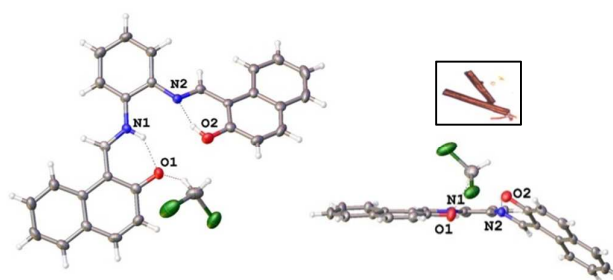


Fig. 1 Projection of [H₂L] and interstitial CH₂Cl₂ solvent molecule. Carbon atoms are shown in grey, nitrogen in blue, oxygen in red, and chlorine in green. Inset image of crystals.

These features speak to the importance of equatorial ligand interactions with the metal centre, and illustrate the profound impacts that subtle differences in the coordination sphere can have on the reactivity of uranium species.

Salophen ligands, which differ from popular salen ligands through the incorporation of a phenylene backbone, thereby extending conjugation, coordinate to the equatorial plane of uranyl through two phenolate and two neutral imine donors. This framework has been popular for studying the structure and reactivity of uranium species, and its redox capabilities have been exploited for C–C bond formation⁶ and the isolation of ligand radical anions.⁷ We have also recently reported complexes of a salophen derivative, 1,1'-((1E,1'E)-(1,2-phenylenebis(azanylylidene))bis(methanylylidene))bis(naphthalen-2-ol), nicknamed “naphthylsalophen”, that exhibit interesting electronic communication aided by extended π -conjugation, including an emissive thorium species.⁸

Here, we take advantage of the features offered by this ligand system to examine the electronic properties of an unusual uranyl complex. The ligand, [H₂L], was prepared from the reaction of two equivalents of 2-hydroxynaphthaldehyde with 1,2-diaminobenzene in methanol. A precipitate formed after heating the solution to 70 °C for four hours and was isolated via vacuum filtration. The product identity was confirmed by ¹H NMR.⁹ The metal complex UO₂[L] was synthesized by addition of UO₂(NO₃)₂•6H₂O to a solution of

^a 179 Chemistry Building, Auburn University, Auburn, AL 36849.

† Footnotes relating to the title and/or authors should appear here.

Electronic Supplementary Information (ESI) available: [experimental details, electronic spectroscopy, crystallographic tables]. See DOI: 10.1039/x0xx00000x

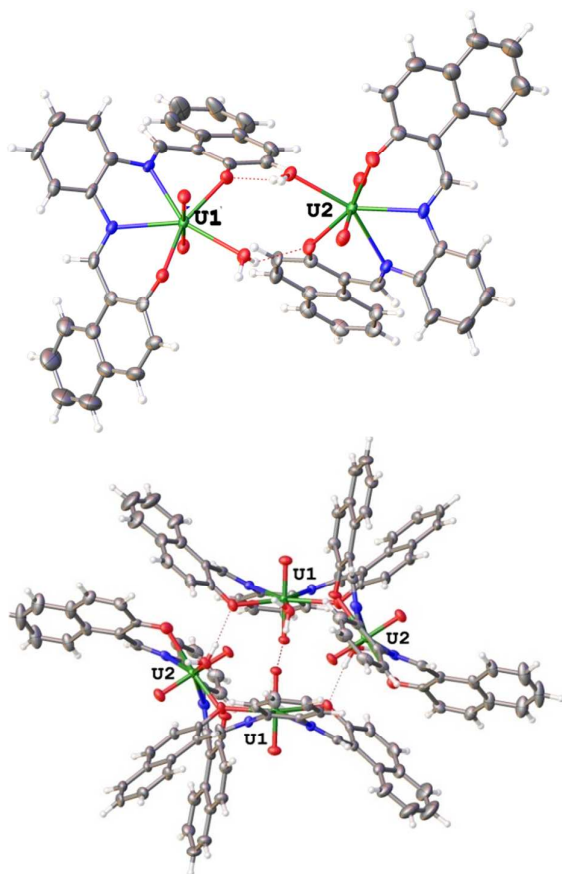


Fig. 2a Projection of the asymmetric unit of $\text{UO}_2[\text{L}]$. **Fig. 2b** Projections of the $\text{UO}_2[\text{L}]$ complex highlighting the hydrogen bonded tetramers. Interstitial CH_2Cl_2 solvent molecules have been removed for clarity. Carbon atoms are shown in grey, oxygen in red, nitrogen in blue, hydrogen in white, and the uranium in green.

$[\text{H}_2\text{L}]$ and trimethylamine dissolved in 1:1 methanol/dichloromethane and subsequent heating. The resulting dark red solid was isolated via vacuum filtration and characterized via NMR, HRMS, and X-ray diffraction (details in SI).

The free base $[\text{H}_2\text{L}]$ has three electronic absorption features at 316 nm ($\epsilon = 9.57 \times 10^3 \text{ cm}^{-1} \text{ M}^{-1}$), 391 nm ($\epsilon = 9.50 \times 10^3 \text{ cm}^{-1} \text{ M}^{-1}$), and 456 nm ($\epsilon = 8.02 \times 10^3 \text{ cm}^{-1} \text{ M}^{-1}$), with a shoulder at 477 nm ($\epsilon = 7.08 \times 10^3 \text{ cm}^{-1} \text{ M}^{-1}$). Deprotonation and coordination to UO_2^{2+} results in a maximum absorbance at 340 nm ($\epsilon = 1.21 \times 10^4 \text{ cm}^{-1} \text{ M}^{-1}$), a shift of 24 nm from the free ligand, and a moderate increase in extinction coefficient. An additional absorption feature is observed at 407 nm ($\epsilon = 8.72 \times 10^3 \text{ cm}^{-1} \text{ M}^{-1}$) with a shoulder at 422 nm ($\epsilon = 7.25 \times 10^3 \text{ cm}^{-1} \text{ M}^{-1}$). A figure showing the change in the UV-Vis signature with the addition of a uranyl nitrate solution by serial titration of $[\text{H}_2\text{L}]$ can be found in Fig. S1. The change observed appears consistent with 1:1 binding.

Single crystals of $\text{[H}_2\text{L]}$ suitable for X-ray diffraction were grown by slow evaporation of a saturated 1:1 dichloromethane/methanol solution. The ligand $[\text{H}_2\text{L}]$

crystallizes in the orthorhombic space group $\text{P}2_12_12_1$ with an interstitial CH_2Cl_2 molecule in the asymmetric unit (Fig. 2). The C—O1 bond length of 1.276(3) and C—O2 bond length of 1.338(3) show that the “ketoamine” tautomer is more stable than the “enolimine” tautomer in the solid-state (Scheme S1). The longer $\text{C}_{\text{imine}}-\text{N}1$ distance of 1.319(3) in comparison to $\text{C}_{\text{imine}}-\text{N}2$ of 1.302(2) also confirms this assignment, although not as clearly. This tautomerization has been observed and explained before for this system in solution using ^1H NMR and IR,¹⁰ as well as crystallographically.⁹

Single crystals of $\text{[UO}_2[\text{L}]$ were grown by slow diffusion of hexanes into a saturated solution of $\text{UO}_2[\text{L}]$ in CH_2Cl_2 . $\text{UO}_2[\text{L}]$ crystallizes in the $\text{P}2_1/n$ space group with four interstitial dichloromethane molecules, and two distinct $\text{UO}_2[\text{L}]$ units per asymmetric unit (Fig. 2a). The average $\text{U}-\text{N}_{\text{imine}}$ bond lengths of 2.515(6) Å, $\text{U}-\text{O}_{\text{H}_2\text{O}}$ bond lengths of 2.450(5) Å, and the $\text{U}-\text{O}_{\text{phenol}}$ bond lengths of 2.286(5) Å are within normal ranges for U(VI) species. Of note is the coordinated water molecule, which participates in hydrogen bonding with one of the phenolic oxygens, resulting in a lengthened $\text{U}-\text{O}_{\text{phenol}}$ distance of 2.311(5) Å, as well as interacts with the -yl oxygen of the neighbouring complex. These two distinct $\text{UO}_2[\text{L}]$ molecules in the asymmetric unit are symmetry-related to two other molecules, resulting in a tetrad of $\text{UO}_2[\text{L}]$ complexes held together through hydrogen bonding interactions. The coordinated water molecule has $\text{H}-\text{O}_{\text{phenol}}$ distances of 1.923 and 2.032 Å, which are within normal ranges, and an $\text{H}\cdots\text{O}_{\text{yl}}$ distance of 2.443 Å. This $\text{H}\cdots\text{O}_{\text{yl}}$ interaction does not qualify as a true hydrogen bond, as the $\text{U}-\text{O}_{\text{yl}}$ distances of 1.795(5) Å and 1.769(5) Å are on par for U(VI)— O_{yl} bonds, however the former does show a slight lengthening. Recent work by Arnold has examined Lewis acid interactions with the -yl oxygen, and in these cases, the reduction of uranyl(VI) to uranyl(V) is confirmed by $\text{U}-\text{O}_{\text{yl}}$ bonds lengths upwards of 1.88 Å,^{4b, c} but such changes are not observed for our system. Additionally, hydrogen atoms on three of the four interstitial CH_2Cl_2 molecules are 2.353 Å, 2.495 Å and 2.528 Å away from the -yl oxygen, the latter two of which interact with opposite ends of the same uranyl unit (Fig. S2). We previously observed similar interactions of CH_2Cl_2 with the uranyl oxo moiety in the presence of a redox-active equatorial ligand,¹¹ however no perturbations of $\text{U}-\text{O}_{\text{yl}}$ bond lengths were observed. The $\text{H}\cdots\text{O}_{\text{yl}}$ distance in this case, which is 0.062 Å shorter, does correspond to the slightly elongated $\text{U}-\text{O}_{\text{yl}}$ bond, indicating the oxo moieties are not entirely inert.

The hydrogen bonding interactions observed in the complex $\text{UO}_2[\text{L}]$, paired with $\pi-\pi$ stacking of the naphthalene rings of 4.304 Å, affords an interesting long-range supramolecular stacking structure with channels that are occupied by interstitial CH_2Cl_2 in the solid-state (Fig. 2b & S2), similar to those observed in metal organic frameworks (MOFs).¹² These stacking interactions are off-set, which is common in structures such as these, but is a consequence of the packing rather than an interaction that would allow this structure to maintain these tetramers in solution and therefore limits their application.

Preliminary electrochemical analysis of $[H_2L]$ and $UO_2[L]$ is reported. Cyclic voltammetry experiments were conducted in acetonitrile (0.1 M $TBAClO_4$ supporting electrolyte), and all values are reported versus the Fc^+/Fc couple. For the free ligand, $[H_2L]$, multiple reductive events were observed (Fig. 3). The irreversible reduction at $E_{pc} = -2.79$ V can be assigned to the $2e^-$ reduction of H_2L to L^{2-} , which is shifted anodically by 100 mV relative to that of salophen¹³ and can be attributed to the extension of the π -conjugated system. The quasireversible reduction at $E_{pc} = -2.90$ V ($E_{pa} = -2.80$ V) corresponds to the formation of the naphthyl radical anion¹⁴ and is associated with the oxidation at -1.67 V, which is not observed unless the scan is conducted to potentials more negative than -2.6 V. The positions and intensities of the peaks at -1.87 , and -2.1 V are scan-rate-dependent (Fig. S4, S5), and could not be assigned definitively, though we posit that while these events are in range for the reduction of H_2L to H_2L^{*} ,^{13a} they may result from the intermolecular H-bonding of the phenolic protons to the imine nitrogens⁹ or tautomerism of the species in solution, as they are not observed in the voltammogram of the uranyl complex. This behaviour is distinct from that of salophen, which undergoes reduction (assigned to the formation of H_2L^{*}) at similar potentials, but does not exhibit the same scan-rate dependence.^{13a}

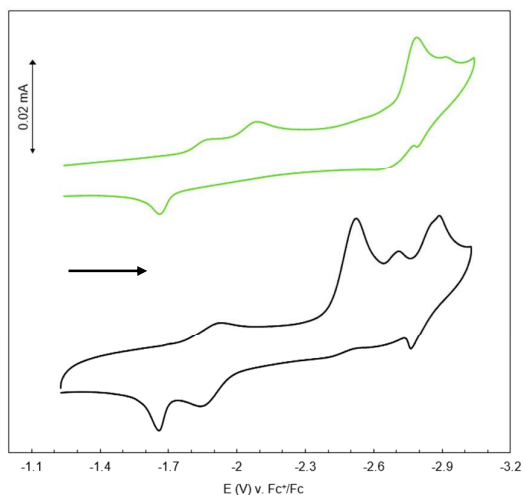


Fig. 3. Cyclic voltammograms of $[H_2L]$ (top) and $UO_2[L]$ (bottom) (0.25 mM in CH_3CN ; 0.1 M $TBAClO_4$, $v=0.2$ V/s).

In the cathodic scan of $UO_2[L]$, four peaks are observed at $E_{pc} = -1.93$ V, -2.53 V, -2.71 V, and -2.89 V. Irreversible reduction of the ligand occurs at -2.53 V (an anodic shift of 260 mV relative to the free ligand), and the quasireversible reduction of the naphthyl substituents is again seen at -2.89 V. Additionally, the oxidation event at $E_{pa} = -1.66$ V is ligand-based and only occurs when the scan is conducted to appreciably cathodic potentials, as observed for the free ligand. The reduction at -1.93 V is quasireversible (though nearly reversible) and associated with the return oxidation event at $E_{pa} = -1.84$ V ($E_{1/2} = -1.89$ V, $\Delta E = 86$ mV) and can be assigned to the $U(VI)/U(V)$ (UO_2^{2+}/UO_2^+) couple. This value

agrees with those previously reported for uranyl salen-type complexes¹⁵, though it is more negative than those reported for $[UO_2(\text{salophen})]$ complexes (*ca.* -1.65 V) and associated with a much smaller ΔE .¹⁶ The irreversible reduction at -2.71 V warrants further investigation as it is in range for the formation of a $L^{2-}-U(IV)$ species,¹⁷ although it overlaps with the reduction of the free ligand to L^{2-} , for which a small shoulder is observed at scan rates greater than 0.3 V/s (Fig. S4), precluding any clear assignment of this process.

It is worth noting that the definition of the $U(VI)/U(V)$ couple appears to be dependent on scanning to more negative potentials and may be associated with the ligand-based reduction at -2.89 V. When the sweep range is limited to more positive potentials, a couple can still be seen but is poorly defined, anodically shifted ($E_{pc} = -1.85$ V, $E_{pa} = -1.76$ V), and includes a shoulder at -1.73 V which is likely associated with a ligand reduction process (Fig. S6). Additionally, a peak at -2.3 V is observed that may correspond to a more drastic anodic shift of the L/L^{2-} reduction potential. These sweep-range-dependent events indicate a significant degree of electronic communication exists between the ligand and the metal centre in solution.

In conclusion, we have synthesized the tetradentate Schiff base ligand, naphthylsalophen $[H_2L]$, and the hexavalent uranyl complex $UO_2[L]$, and characterized them in solution and solid-state. Interactions of coordinated water and solvent protons with the uranyl oxo moiety result in a slight elongation of the $U-O_{yl}$ bond in the solid state. The fairly complex electrochemical profile and observed 260 mV shift in the ligand reduction potential is evidence that this derivative of the thoroughly studied uranyl salophen system possesses interesting redox behaviour that is usually observed only with more specialized redox-active ligands, and is thus, of interest for further investigations with particular interest in any oxo reactivity it may exhibit. These findings speak to the intricacies of $5f$ metal-ligand interactions and highlight the need to of the fundamental behaviour of the actinides.

Conflicts of interest

There are no conflicts to declare.

Acknowledgements

We would like to thank Prof. Byron Farnum and members of the Farnum lab for the use of their potentiostat and helpful discussions. This work was supported by the Defense Threat Reduction Agency, Basic Research Award #HDTRA1-11-1-0044, to Auburn University.

Notes and references

#Crystal Data for $[H_2L]$ $C_{29}H_{22}Cl_2N_2O_2$ ($M = 501.42$): orthorhombic, space group $P2_12_12_1$ (no. 19), $a = 7.1378(10)$ Å, $b = 16.682(2)$ Å, $c = 20.056(3)$ Å, $V = 2388.1(6)$ Å³, $Z = 4$, $T = 180.45$ K, $\mu(\text{Mo K}\alpha) = 0.303$ mm⁻¹, $D_{calc} = 1.3945$ g/mm³, 17603 reflections measured ($4.06 \leq 2\theta \leq 57.4$), 6177 unique ($R_{int} = 0.0539$, $R_{sigma} = 0.0733$) which were used in all calculations. The final R_1 was 0.0557 ($I \geq 2\sigma(I)$) and wR_2 was 0.1295 (all data). CCDC: 1523762. Crystal Data for $UO_2[L]$: $C_{60}H_{48}Cl_8N_4O_{10}U_2$ ($M = 1744.75$): monoclinic, space group $P2_1/n$

(no. 14), $a = 15.4659(12) \text{ \AA}$, $b = 19.3294(14) \text{ \AA}$, $c = 22.2346(16) \text{ \AA}$, $\beta = 106.655(1)^\circ$, $V = 6368.1(8) \text{ \AA}^3$, $Z = 4$, $T = 180.0 \text{ K}$, $\mu(\text{Mo K}\alpha) = 5.476 \text{ mm}^{-1}$, $D_{\text{calc}} = 1.8197 \text{ g/mm}^3$, 74217 reflections measured ($2.84 \leq 2\theta \leq 51.52$), 12168 unique ($R_{\text{int}} = 0.0706$, $R_{\text{sigma}} = 0.0463$) which were used in all calculations. The final R_1 was 0.0440 ($I \geq 2\sigma(I)$) and wR_2 was 0.1031 (all data). CCDC: 1827293.

- Mizuoka, S.-Y. Kim, M. Hasegawa, T. Hoshi, G. Uchiyama and Y. Ikeda, *Inorg. Chem.*, 2003, **42**, 1031-1038.
17. J. R. Pankhurst, N. L. Bell, M. Zegke, L. N. Platts, C. A. Lamfsus, L. Maron, L. S. Natrajan, S. Sproules, P. L. Arnold and J. B. Love, *Chem. Sci.*, 2017, **8**, 108-116.

- (a) A. R. Fox, S. C. Bart, K. Meyer and C. C. Cummins, *Nature*, 2008, **455**, 341; (b) D. P. Halter, F. W. Heinemann, J. Bachmann and K. Meyer, *Nature*, 2016, **530**, 317.
- J. C. Renshaw, L. J. C. Butchins, F. R. Livens, I. May, J. M. Charnock and J. R. Lloyd, *Environ. Sci. Technol.*, 2005, **39**, 5657-5660.
- (a) L. A. Seaman, E. A. Pedrick, G. Wu and T. W. Hayton, *Journal of Organometallic Chemistry*, 2018, **857**, 34-37; (b) B. E. Cowie, G. S. Nichol, J. B. Love and P. L. Arnold, *Chem. Comm.*, 2018, **54**, 3839-3842.
- (a) T. W. Hayton and G. Wu, *Inorg. Chem.*, 2009, **48**, 3065-3072; (b) P. L. Arnold, E. Hollis, G. S. Nichol, J. B. Love, J.-C. Griveau, R. Caciuffo, N. Magnani, L. Maron, L. Castro, A. Yahia, S. O. Odoh and G. Schreckenbach, *J. Am. Chem. Soc.*, 2013, **135**, 3841-3854; (c) P. L. Arnold, A.-F. Pécharman, R. M. Lord, G. M. Jones, E. Hollis, G. S. Nichol, L. Maron, J. Fang, T. Davin and J. B. Love, *Inorg. Chem.*, 2015, **54**, 3702-3710.
- N. L. Bell, B. Shaw, P. L. Arnold and J. B. Love, *J. Am. Chem. Soc.*, 2018, **140**, 3378-3384.
- C. Camp, D. Toniolo, J. Andrez, J. Pecaut and M. Mazzanti, *Dalton. Trans.*, 2017, **46**, 11145-11148.
- K. Herasymchuk, L. Chiang, C. E. Hayes, M. L. Brown, J. S. Owens, B. O. Patrick, D. B. Leznoff and T. Storr, *Dalton. Trans.*, 2016, **45**, 12576-12586.
- (a) E. E. Hardy, K. M. Wyss, J. D. Gorden, I. R. Ariyaratna, E. Miliordos and A. E. V. Gorden, *Chem. Comm.*, 2017, **53**, 11984-11987; (b) E. E. Hardy, K. M. Wyss, R. J. Keller, J. D. Gorden and A. E. V. Gorden, *Dalton. Trans.*, 2018, **47**, 1337-1346.
- Z. Popović, V. Roje, G. Pavlović, D. Matković-Čalogović and G. Giester, *Journal of Molecular Structure*, 2001, **597**, 39-47.
- V. Z. Mota, G. S. G. de Carvalho, P. P. Corbi, F. R. G. Bergamini, A. L. B. Formiga, R. Diniz, M. C. R. Freitas, A. D. da Silva and A. Cuin, *Spectrochim. Acta, Part A*, 2012, **99**, 110-115.
- J. E. Niklas, B. H. Farnum, J. D. Gorden and A. E. V. Gorden, *Organometallics*, 2017, **36**, 4626-4634.
- (a) Z. Hao, X. Song, M. Zhu, X. Meng, S. Zhao, S. Su, W. Yang, S. Song and H. Zhang, *Journal of Materials Chemistry A*, 2013, **1**, 11043-11050; (b) Y. Wang, Z. Liu, Y. Li, Z. Bai, W. Liu, Y. Wang, X. Xu, C. Xiao, D. Sheng, J. Diwu, J. Su, Z. Chai, T. E. Albrecht-Schmitt and S. Wang, *J. Am. Chem. Soc.*, 2015, **137**, 6144-6147.
- (a) A. A. Isse, A. Gennaro and E. Vianello, *Electrochimica Acta*, 1997, **42**, 2065-2071; (b) C. Camp, V. Guidal, B. Biswas, J. Pecaut, L. Dubois and M. Mazzanti, *Chem. Sci.*, 2012, **3**, 2433-2448.
- N. V. Vasilieva, I. G. Irtegova, T. A. Vaganova and V. D. Shteingarts, *J. Phys. Org. Chem.*, 2008, **21**, 73-78.
- S.-Y. Kim, H. Tomiyasu and Y. Ikeda, *J. Nucl. Sci. Technol.*, 2002, **39**, 160-165.
- (a) G. Nocton, P. Horeglad, V. Vetere, J. Pécaut, L. Dubois, P. Maldivi, N. M. Edelstein and M. Mazzanti, *J. Am. Chem. Soc.*, 2010, **132**, 495-508; (b) P. L. Arnold, G. M. Jones, Q.-J. Pan, G. Schreckenbach and J. B. Love, *Dalton. Trans.*, 2012, **41**, 6595-6597; (c) T. W. Hayton, J. M. Boncella, B. L. Scott, E. R. Batista and P. J. Hay, *J. Am. Chem. Soc.*, 2006, **128**, 10549-10559; (d) K.